RADIOCARBON, Vol 46, Nr 3, 2004, p 1211–1224

RADIOCARBON RESULTS FROM A 13-KYR BP CORAL FROM THE HUON PENINSULA, PAPUA NEW GUINEA

G S Burr[1] • Chrystie Galang[1] • F W Taylor[2] • Christina Gallup[3] • R Lawrence Edwards[4] • Kirsten Cutler[4] • Bill Quirk[5]

ABSTRACT. This paper presents radiocarbon results from a single *Goniastrea favulus* coral from Papua New Guinea which lived continuously between 13.0 and 13.1 kyr BP. The specimen was collected from a drill core on the Huon Peninsula and has been independently dated with ^{230}Th. A site-specific reservoir correction has been applied to the results, and coral growth bands were used to calibrate individual growth years. Alternating density bands, which are the result of seasonal growth variations, were subsampled to provide 2 integrated 6-month ^{14}C measurements per year. This allows for 20 independent measurements to be averaged for each decadal value of the ^{14}C calibration, making these results the highest resolution data set available for this brief time range. The finestructure of the data set exhibits ^{14}C oscillations with frequencies on the order of 4 to 10 yr, similar to those observed in modern coral ^{14}C records.

INTRODUCTION

Radiocarbon dates may be calibrated using a variety of natural archives. The IntCal98 calibration combines tree rings, corals, and marine varved sediments (Stuiver et al. 1998), and the same combination is applied in the present IntCal04 calibration (Reimer et al., this issue). Tree rings provide the most robust results, with potentially annual temporal resolution, but they are limited to trees which can be wiggle-matched to known years. Corals, dated with U/Th, were first utilized by Bard et al. (1990, 1993, 1996) to extend the tree-ring limit of the ^{14}C calibration. One potential advantage of corals is that the skeletons of some species preserve subannual chemical variations related to seawater chemistry, and have relatively thick and continuous growth bands. Certain of these species can also live for hundreds of years. These features of coral archives have been widely exploited over the past 2 decades to produce a wealth of climate data from oxygen isotopic and trace element analyses (Druffel 1997; Gagan et al. 2000). However, there has only been 1 example of a single long-lived coral applied to the ^{14}C calibration. This is the *Diploastrea heliopora* analyzed as part of the IntCal98 effort. The *Diploastrea* was collected from Vanuatu and preserved a ^{14}C record spanning more than 400 yr during the Younger Dryas (Burr et al. 1998). Two reasons why more corals of this type are not available are the rare geologic conditions required for their preservation and the logistical difficulties which must be overcome to collect them. The *Diploastrea* sample grew in a tectonically active region off the coast of Espiritu Santo Island in Vanuatu. This site is located along a plate boundary that has experienced rapid and variable uplift since the time the coral lived there (Taylor et al. 1987; Cabioch et al. 2003). The amount and direction of tectonic uplift in Vanuatu matched the concurrent rapid sea-level rise during this period, leaving the coral in a position where it could be retrieved by drilling. As there is no existing technology which can locate large buried coral heads, it was also fortuitous that the position of the drill rig during the Vanuatu field campaign happened to be located over this particular coral. Such fortunate circumstances have not often been repeated at other sites and such samples remain rare.

[1]University of Arizona, NSF-Arizona AMS Laboratory, Tucson, Arizona 85721, USA.
[2]Institute for Geophysics, The University of Texas at Austin, 4412 Spicewood Springs Road, Bld. 600, Austin, Texas 78759-8500, USA.
[3]University of Minnesota Duluth Geological Sciences, Room 229 HHD175, 10 University Drive, Duluth, Minnesota 55812, USA
[4]Minnesota Isotope Laboratory, Department of Geology and Geophysics, University of Minnesota, 310 Pillsbury Drive SE, Minneapolis, Minnesota 55455, USA.
[5]University Medical Center, University of Arizona, Tucson, Arizona 85721, USA.

We report here on another such coral, which lived for about a century between 13.0 and 13.1 kyr BP. This coral is a *Goniastrea favulus* and was collected during a drilling campaign in 1996. The drilling took place on an uplifted Holocene terrace located on the Huon Peninsula in Papua New Guinea (Figure 1). The drill was positioned a few meters from the present shoreline, near Kwambu Village, and the sample was encountered at about 40 m depth. The tectonic setting of the Huon Peninsula is similar to Vanuatu, experiencing continual and rapid uplift throughout the Holocene (Chappell and Polach 1991), and the reef was able to keep up with the approximately 100 m of sea-level rise which occurred during the last 13 kyr (Cutler et al. 2003).

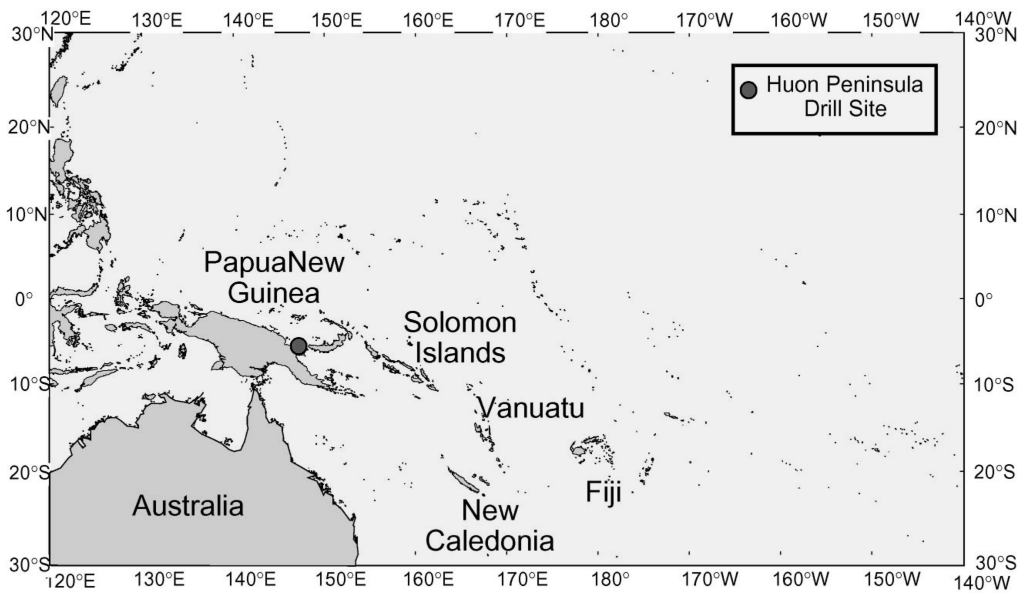

Figure 1 Location of drill site used to collect the sample

METHODS

A 1.5-inch-diameter core was drilled perpendicular to the vertical growth axis of the *Goniastrea favulus*. This was cut in half lengthwise with a diamond saw and then cut again to into a 5-mm slab. The slab was X-rayed to identify individual growth bands (Figure 2). The X-ray image reveals sub-annual high- and low-density bands. Each pair of high- and low-density bands accounts for 1 yr of growth. An advantage of using this species of coral is that it produces very well-defined density bands as is evident in Figure 2. Two samples were taken for each year of growth—a low-density subsample and a high-density subsample. The sampling was carefully conducted so as to collect the entire light or dark band as viewed in the X-ray image. This was done to obtain an integral ^{14}C measurement for the approximately 6-month growth period and thus average higher frequency ^{14}C variations, which are known to occur in corals (Brown et al. 1993; Moore et al. 1997; Guilderson et al. 1998).

Each sample was dissolved in acid to produce CO_2, and the gas was subsequently reduced to graphite for accelerator mass spectrometry (AMS) analysis. All of the samples were subjected to the selective dissolution technique described by Burr et al. (1992). A piece of the core was analyzed using X-ray powder diffraction to ensure that it was free of secondary calcite. Multiple measurements of corals in excess of 100 kyr were used to determine the blank and blank uncertainty. A discussion of the background calculation is given in Donahue et al. (1990).

Figure 2 X-ray image of the *Goniastrea favulus* sample. Note the alternating light and dark density bands. The core is approximately 1.5 inches in diameter.

RESULTS AND DISCUSSION

All of the results presented here are given as fraction modern carbon (F) values, reservoir-corrected fraction modern carbon (F_{RC}) values, and reservoir-corrected ^{14}C ages and ^{14}C values. F is defined by the equation

$$F = (^{14}C/^{13}C)_S / (^{14}C/^{13}C)_{STD} ,$$

where $(^{14}C/^{13}C)_S$ is the sample ratio normalized to $\delta^{13}C = -25‰$ and $(^{14}C/^{13}C)_{STD}$ is the calculated standard ratio at 1950, determined from measurements of NBS oxalic acid standards, also normalized to $\delta^{13}C = -25‰$ (Donahue et al. 1990). Uncorrected F values must be reservoir-corrected with a site-specific reservoir-correction factor to calculate ^{14}C ages that reflect the atmospheric ^{14}C content (equivalent to tree-ring dates). The reservoir-corrected fraction modern carbon F_{RC} is defined here as

$$F_{RC} \equiv Fe^{RC/\tau} ,$$

where RC is the site-specific reservoir correction in years and τ is the Libby mean life (8033 yr). For the Huon Peninsula, RC is equal to 407 ± 52 yr (2 σ) (Edwards et al. 1993). This value was chosen because these samples came from the same site studied by Edwards et al. (1993). The uncertainty in the reservoir correction is propagated into the total uncertainty of each measurement (uncorrected F value) to yield the uncertainty in F_{RC}, according to the equation (Burr et al. 1998):

$$\sigma_{F_{RC}} = \left\{(e^{(RC)/\tau})^2(\sigma_F)^2 + [(F/\tau)(e^{(RC)/\tau})]^2(\sigma_{RC})^2\right\}^{\frac{1}{2}} .$$

The σs represent the uncertainties in F_{RC}, F, and RC.

$\Delta^{14}C$ values were computed from F_{RC} values using the relation

$$\Delta^{14}C = (F_{RC}\, e^{\lambda t} - 1)\ 1000‰ ,$$

where t is the age BP of the sample in calendar years.

The total uncertainty in $\Delta^{14}C$ is σ_Δ and includes errors in F_{RC} and in the ^{230}Th ages (t), according to the expression

$$\sigma_\Delta = 1000e^{\lambda t}[(F_{RC}\lambda)^2\sigma_t^2 + \sigma_{F_{RC}}^2]^{\frac{1}{2}} .$$

Table 1 gives the results of the ^{230}Th measurements. Three independent measurements were made at the Minnesota Isotope Laboratory and all of them are internally consistent. Table 2 lists the biannual ^{14}C results for each growth year and assigns a corresponding calendar age to these, according to the ^{230}Th results. These data are summarized as 5-yr weighted averages in Table 3.

Table 1 ^{230}Th results.

Sample	^{238}U (ppb)	^{232}Th (pg/g)	$^{230}Th/^{238}U$ (activity)	$\delta^{234}U_m$ (‰)	^{230}Th age BP (kyr) before 1950	$\delta^{234}U_i$ (‰)
PNG-96-41.27-88[a]	2166.2 ± 2.9	123.4 ± 5.5	0.12892 ± 0.00037	142.8 ± 1.7	12,985 ± 45	148.2 ± 1.7
replicate analysis					12,996 ± 129	
PNG-96-41.27-11	1383.5 ± 1.8	9.0 ± 2.4	0.13015 ± 0.00035	143.0 ± 1.6	13,115 ± 43	148.4 ± 1.7
Average date of the core top: 13,011 ± 30 (2 σ)						

[a]There are 88 yr of growth preserved. Layer #88 is the uppermost dark/light band couplet.

Table 2 Calibrated ^{14}C results—biannual data.

Lab # AA-	Sample ID	$\delta^{13}C$	^{230}Th age	±2 σ	F	±1 σ	F_{RC}	±1 σ	^{14}C age BP	±2 σ
AA52727	PNG 96 41.27 11D	0.2	13,088.5	30.0	0.2441	0.0019	0.2568	0.0022	10,921	135
AA52728	PNG 96 41.27 11L	–0.8	13,088.0	30.0	0.2385	0.0014	0.2509	0.0017	11,107	108
AA52729	PNG 96 41.27 12D	–0.1	13,087.5	30.0	0.2381	0.0016	0.2505	0.0019	11,121	120
AA52730	PNG 96 41.27 12L	0.1	13,087.0	30.0	0.2352	0.0013	0.2474	0.0016	11,219	103
AA52731	PNG 96 41.27 13D	–0.1	13,086.5	30.0	0.2380	0.0018	0.2504	0.0021	11,124	132
AA52732	PNG 96 41.27 13L	–0.6	13,086.0	30.0	0.2403	0.0019	0.2528	0.0022	11,047	137
AA52733	PNG 96 41.27 14D	0.3	13,085.5	30.0	0.2375	0.0023	0.2498	0.0026	11,141	164
AA52734	PNG 96 41.27 14L	–0.1	13,085.0	30.0	0.2411	0.0014	0.2536	0.0017	11,020	107
AA52735	PNG 96 41.27 15D	0.1	13,084.5	30.0	0.2383	0.0018	0.2507	0.0021	11,114	132
AA52736	PNG 96 41.27 15L	0.8	13,084.0	30.0	0.2415	0.0025	0.2541	0.0028	11,007	174
AA52737	PNG 96 41.27 16D	–0.2	13,083.5	30.0	0.2401	0.0034	0.2526	0.0037	11,054	233
AA52738	PNG 96 41.27 16L	0.6	13,083.0	30.0	0.2392	0.0015	0.2516	0.0018	11,084	113
AA52739	PNG 96 41.27 17D	0.3	13,082.5	30.0	0.2392	0.0018	0.2516	0.0021	11,084	132
AA52740	PNG 96 41.27 17L	0.8	13,082.0	30.0	0.2385	0.0015	0.2509	0.0018	11,107	114
AA52741	PNG 96 41.27 18D	0.4	13,081.5	30.0	0.2376	0.0017	0.2499	0.0020	11,138	126
AA52742	PNG 96 41.27 18L	1.3	13,081.0	30.0	0.2369	0.0022	0.2492	0.0025	11,161	158
AA52743	PNG 96 41.27 19D	0.5	13,080.5	30.0	0.2465	0.0050	0.2593	0.0053	10,842	330
AA52744	PNG 96 41.27 19L	0.9	13,080.0	30.0	0.2429	0.0015	0.2555	0.0018	10,961	112
AA52745	PNG 96 41.27 20D	0.2	13,079.5	30.0	0.2387	0.0014	0.2511	0.0017	11,101	108
AA52746	PNG 96 41.27 20L	0.3	13,079.0	30.0	0.2451	0.0016	0.2578	0.0019	10,888	117
AA52747	PNG 96 41.27 21D	0.3	13,078.5	30.0	0.2410	0.0014	0.2535	0.0017	11,024	107
AA52748	PNG 96 41.27 21L	0.3	13,078.0	30.0	0.2418	0.0015	0.2544	0.0018	10,997	112
AA52749	PNG 96 41.27 22D	0.1	13,077.5	30.0	0.2402	0.0014	0.2527	0.0017	11,050	107
AA52750	PNG 96 41.27 22L	0.6	13077.0	30.0	0.2406	0.0019	0.2531	0.0022	11,037	137
AA52751	PNG 96 41.27 23D	0.4	13,076.5	30.0	0.2402	0.0014	0.2527	0.0017	11,050	107
AA52752	PNG 96 41.27 23L	0.4	13,076.0	30.0	0.2385	0.0014	0.2509	0.0017	11,107	108
AA52753	PNG 96 41.27 24D	1.3	13,075.5	30.0	0.2397	0.0014	0.2522	0.0017	11,067	107
AA52754	PNG 96 41.27 24L	0.5	13,075.0	30.0	0.2447	0.0014	0.2574	0.0017	10,901	106
AA52755	PNG 96 41.27 25D	0.0	13,074.5	30.0	0.2403	0.0014	0.2528	0.0017	11,047	107
AA52756	PNG 96 41.27 25L	–0.1	13,074.0	30.0	0.2447	0.0014	0.2574	0.0017	10,901	106
AA52757	PNG 96 41.27 26D	0.1	13,073.5	30.0	0.2446	0.0016	0.2573	0.0019	10,905	117

Table 2 Calibrated ^{14}C results—biannual data. *(Continued)*

Lab # AA-	Sample ID	$\delta^{13}C$	^{230}Th age	±2 σ	*F*	±1 σ	F_{RC}	±1 σ	^{14}C age BP	±2 σ
AA52758	PNG 96 41.27 26L	0.0	13,073.0	30.0	0.2415	0.0014	0.2541	0.0017	11,007	107
AA52759	PNG 96 41.27 27D	0.5	13,072.5	30.0	0.2451	0.0017	0.2578	0.0020	10,888	123
AA52760	PNG 96 41.27 27L	0.0	13,072.0	30.0	0.2439	0.0015	0.2566	0.0018	10,928	112
AA52761	PNG 96 41.27 28D	0.0	13,071.5	30.0	0.2539	0.0024	0.2671	0.0027	10,605	161
AA52762	PNG 96 41.27 28L	0.2	13,071.0	30.0	0.2451	0.0017	0.2578	0.0020	10,888	123
AA52763	PNG 96 41.27 29D	0.0	13,070.5	30.0	0.2421	0.0019	0.2547	0.0022	10,987	136
AA52764	PNG 96 41.27 29L	0.0	13,070.0	30.0	0.2374	0.0016	0.2497	0.0019	11,145	120
AA52765	PNG 96 41.27 30D	0.5	13,069.5	30.0	0.2374	0.0015	0.2497	0.0018	11,145	114
AA52766	PNG 96 41.27 30L	0.6	13,069.0	30.0	0.2387	0.0014	0.2511	0.0017	11,101	108
AA52767	PNG 96 41.27 31D	0.6	13,068.5	30.0	0.2424	0.0014	0.2550	0.0017	10,977	106
AA52768	PNG 96 41.27 31L	0.1	13,068.0	30.0	0.2383	0.0014	0.2507	0.0017	11,114	108
AA52769	PNG 96 41.27 32D	0.2	13,067.5	30.0	0.2444	0.0028	0.2571	0.0031	10,911	191
AA52770	PNG 96 41.27 32L	–0.3	13,067.0	30.0	0.2361	0.0014	0.2484	0.0017	11,189	109
AA52771	PNG 96 41.27 33D	–0.2	13,066.5	30.0	0.2384	0.0014	0.2508	0.0017	11,111	108
AA52772	PNG 96 41.27 33L	–0.3	13,066.0	30.0	0.2336	0.0015	0.2457	0.0018	11,274	116
AA52773	PNG 96 41.27 34D	0.0	13,065.5	30.0	0.2350	0.0014	0.2472	0.0017	11,226	109
AA52774	PNG 96 41.27 34L	–0.2	13,065.0	30.0	0.2385	0.0014	0.2509	0.0017	11,107	108
AA52775	PNG 96 41.27 35D	0.3	13,064.5	30.0	0.2400	0.0017	0.2525	0.0020	11,057	125
AA52776	PNG 96 41.27 35L	0.0	13,064.0	30.0	0.2382	0.0017	0.2506	0.0020	11,118	126
AA52777	PNG 96 41.27 36D	0.5	13,063.5	30.0	0.2379	0.0017	0.2503	0.0020	11,128	126
AA52778	PNG 96 41.27 36L	0.2	13,063.0	30.0	0.2363	0.0017	0.2486	0.0020	11,182	127
AA52779	PNG 96 41.27 37D	0.3	13,062.5	30.0	0.2366	0.0014	0.2489	0.0017	11,172	108
AA52780	PNG 96 41.27 37L	–0.2	13,062.0	30.0	0.2410	0.0014	0.2535	0.0017	11,024	107
AA52781	PNG 96 41.27 38D	0.0	13,061.5	30.0	0.2373	0.0014	0.2496	0.0017	11,148	108
AA52782	PNG 96 41.27 38L	0.2	13,061.0	30.0	0.2391	0.0018	0.2515	0.0021	11,087	132
AA52783	PNG 96 41.27 39D	0.0	13,060.5	30.0	0.2378	0.0015	0.2502	0.0018	11,131	114
AA52784	PNG 96 41.27 39L	–0.1	13,060.0	30.0	0.2370	0.0014	0.2493	0.0017	11,158	108
AA52785	PNG 96 41.27 40D	0.1	13,059.5	30.0	0.2420	0.0015	0.2546	0.0018	10,990	112
AA52786	PNG 96 41.27 40L	–0.3	13,059.0	30.0	0.2373	0.0022	0.2496	0.0025	11,148	158
AA52787	PNG 96 41.27 41D	0.3	13,058.5	30.0	0.2365	0.0016	0.2488	0.0019	11,175	120
AA52788	PNG 96 41.27 41L	–0.2	13,058.0	30.0	0.2383	0.0014	0.2507	0.0017	11,114	108

Table 2 Calibrated ^{14}C results—biannual data. *(Continued)*

Lab # AA-	Sample ID	$\delta^{13}C$	^{230}Th age	±2 σ	F	±1 σ	F_{RC}	±1 σ	^{14}C age BP	±2 σ
AA52789	PNG 96 41.27 42D	0.6	13,057.5	30.0	0.2514	0.0021	0.2645	0.0024	10,684	144
AA52790	PNG 96 41.27 42L	–0.1	13,057.0	30.0	0.2417	0.0016	0.2543	0.0019	11,000	118
AA52791	PNG 96 41.27 43D	–0.3	13,056.5	30.0	0.2372	0.0037	0.2495	0.0040	11,151	256
AA52792	PNG 96 41.27 43L	–0.1	13,056.0	30.0	0.2387	0.0024	0.2511	0.0027	11,101	170
AA52793	PNG 96 41.27 44D	0.4	13,055.5	30.0	0.2385	0.0016	0.2509	0.0019	11,107	120
AA52794	PNG 96 41.27 44L	–0.2	13,055.0	30.0	0.2387	0.0023	0.2511	0.0026	11,101	163
AA52795	PNG 96 41.27 45D	0.2	13,054.5	30.0	0.2411	0.0018	0.2536	0.0021	11,020	131
AA52796	PNG 96 41.27 45L	0.2	13,054.0	30.0	0.2381	0.0019	0.2505	0.0022	11,121	138
AA52797	PNG 96 41.27 46D	–0.3	13,053.5	30.0	0.2415	0.0016	0.2541	0.0019	11,007	118
AA52798	PNG 96 41.27 46L	0.0	13,053.0	30.0	0.2416	0.0015	0.2542	0.0018	11,004	112
AA52799	PNG 96 41.27 47D	0.6	13,052.5	30.0	0.2420	0.0018	0.2546	0.0021	10,990	130
AA52800	PNG 96 41.27 47L	0.3	13,052.0	30.0	0.2391	0.0016	0.2515	0.0019	11,087	119
AA52801	PNG 96 41.27 48D	0.1	13,051.5	30.0	0.2393	0.0029	0.2517	0.0032	11,080	202
AA52802	PNG 96 41.27 48L	0.6	13,051.0	30.0	0.2379	0.0013	0.2503	0.0016	11,128	102
AA52803	PNG 96 41.27 49D	0.1	13,050.5	30.0	0.2388	0.0018	0.2512	0.0021	11,097	132
AA52804	PNG 96 41.27 49L	0.3	13,050.0	30.0	0.2373	0.0020	0.2496	0.0023	11,148	145
AA52805	PNG 96 41.27 50D	–0.1	13,049.5	30.0	0.2379	0.0015	0.2503	0.0018	11,128	114
AA52806	PNG 96 41.27 50L	0.0	13,049.0	30.0	0.2425	0.0046	0.2551	0.0049	10,974	309
AA52807	PNG 96 41.27 51D	–0.5	13,048.5	30.0	0.2386	0.0023	0.2510	0.0026	11,104	163
AA52808	PNG 96 41.27 51L	0.0	13,048.0	30.0	0.2385	0.0016	0.2509	0.0019	11,107	120
AA52809	PNG 96 41.27 52D	0.4	13,047.5	30.0	0.2374	0.0015	0.2497	0.0018	11,145	114
AA52810	PNG 96 41.27 52L	0.1	13,047.0	30.0	0.2379	0.0015	0.2503	0.0018	11,128	114
AA52811	PNG 96 41.27 53D	0.3	13,046.5	30.0	0.2393	0.0017	0.2517	0.0020	11,080	125
AA52812	PNG 96 41.27 53L	0.4	13,046.0	30.0	0.2393	0.0018	0.2517	0.0021	11,080	132
AA52813	PNG 96 41.27 54D	–0.1	13,045.5	30.0	0.2389	0.0015	0.2513	0.0018	11,094	113
AA52814	PNG 96 41.27 54L	0.5	13,045.0	30.0	0.2373	0.0017	0.2496	0.0020	11,148	126
AA52815	PNG 96 41.27 55D	0.0	13,044.5	30.0	0.2371	0.0013	0.2494	0.0016	11,155	102
AA52816	PNG 96 41.27 55L	0.4	13,044.0	30.0	0.2391	0.0017	0.2515	0.0020	11,087	126
AA52817	PNG 96 41.27 56D	0.0	13,043.5	30.0	0.2439	0.0030	0.2566	0.0033	10,928	204
AA52818	PNG 96 41.27 57L	–0.1	13,043.0	30.0	0.2487	0.0017	0.2616	0.0020	10,771	122
AA52819	PNG 96 41.27 57D	–0.1	13,042.5	30.0	0.2381	0.0018	0.2505	0.0021	11,121	132

Table 2 Calibrated ^{14}C results—biannual data. *(Continued)*

Lab # AA-	Sample ID	$\delta^{13}C$	^{230}Th age	±2 σ	F	±1 σ	F_{RC}	±1 σ	^{14}C age BP	±2 σ
AA52820	PNG 96 41.27 57L	0.4	13,042.0	30.0	0.2396	0.0021	0.2521	0.0024	11,070	150
AA52821	PNG 96 41.27 58D	–0.5	13,041.5	30.0	0.2394	0.0020	0.2518	0.0023	11,077	144
AA52822	PNG 96 41.27 58L	0.0	13,041.0	30.0	0.2386	0.0016	0.2510	0.0019	11,104	120
AA52823	PNG 96 41.27 59D	–0.5	13,040.5	30.0	0.2378	0.0017	0.2502	0.0020	11,131	126
AA52824	PNG 96 41.27 59L	–0.1	13,040.0	30.0	0.2385	0.0017	0.2509	0.0020	11,107	126
AA52825	PNG 96 41.27 60D	–0.4	13,039.5	30.0	0.2415	0.0018	0.2541	0.0021	11,007	131
AA52826	PNG 96 41.27 60L	–0.3	13,039.0	30.0	0.2389	0.0021	0.2513	0.0024	11,094	150
AA52827	PNG 96 41.27 61D	–0.8	13,038.5	30.0	0.2406	0.0016	0.2531	0.0019	11,037	119
AA52828	PNG 96 41.27 61L	–0.3	13,038.0	30.0	0.2351	0.0015	0.2473	0.0018	11,223	115
AA52829	PNG 96 41.27 62D	–0.7	13,037.5	30.0	0.2415	0.0015	0.2541	0.0018	11,007	113
AA52830	PNG 96 41.27 62L	–0.2	13,037.0	30.0	0.2375	0.0017	0.2498	0.0020	11,141	126
AA52831	PNG 96 41.27 63D	–0.7	13,036.5	30.0	0.2395	0.0014	0.2519	0.0017	11,074	107
AA52832	PNG 96 41.27 63L	–0.5	13,036.0	30.0	0.2372	0.0031	0.2495	0.0034	11,151	216
AA52833	PNG 96 41.27 64D	–0.7	13,035.5	30.0	0.2390	0.0014	0.2514	0.0017	11,091	108
AA52834	PNG 96 41.27 64L	–0.9	13,035.0	30.0	0.2406	0.0029	0.2531	0.0032	11,037	201
AA52835	PNG 96 41.27 65D	–0.8	13,034.5	30.0	0.2378	0.0015	0.2502	0.0018	11,131	114
AA52836	PNG 96 41.27 65L	–0.1	13,034.0	30.0	0.2435	0.0025	0.2562	0.0028	10,941	173
AA52837	PNG 96 41.27 66D	–1.0	13,033.5	30.0	0.2473	0.0014	0.2602	0.0017	10,816	105
AA52838	PNG 96 41.27 66L	1.3	13,033.0	30.0	0.2428	0.0019	0.2554	0.0022	10,964	136
AA52839	PNG 96 41.27 67D	–1.0	13,032.5	30.0	0.2535	0.0023	0.2667	0.0026	10,617	155
AA52840	PNG 96 41.27 67L	–0.1	13,032.0	30.0	0.2374	0.0033	0.2497	0.0036	11,145	229
AA52841	PNG 96 41.27 68D	–0.4	13,031.5	30.0	0.2449	0.0018	0.2576	0.0021	10,895	129
AA52842	PNG 96 41.27 68L	0.3	13,031.0	30.0	0.2421	0.0021	0.2547	0.0024	10,987	149
AA52843	PNG 96 41.27 69D	0.5	13,030.5	30.0	0.2403	0.0017	0.2528	0.0020	11,047	125
AA52844	PNG 96 41.27 69L	0.6	13,030.0	30.0	0.2404	0.0015	0.2529	0.0018	11,044	113
AA52845	PNG 96 41.27 70D	1.0	13,029.5	30.0	0.2418	0.0019	0.2544	0.0022	10,997	137
AA52846	PNG 96 41.27 70L	0.1	13,029.0	30.0	0.2399	0.0014	0.2524	0.0017	11,060	107
AA52847	PNG 96 41.27 71D	–0.3	13,028.5	30.0	0.2471	0.0020	0.2599	0.0023	10,823	140
AA52848	PNG 96 41.27 71L	0.1	13,028.0	30.0	0.2401	0.0017	0.2526	0.0020	11,054	125
AA52849	PNG 96 41.27 72D	–0.9	13,027.5	30.0	0.2394	0.0016	0.2518	0.0019	11,077	119
AA52850	PNG 96 41.27 72L	0.0	13,027.0	30.0	0.2391	0.0016	0.2515	0.0019	11,087	119
AA52851	PNG 96 41.27 73D	–0.7	13,026.5	30.0	0.2418	0.0019	0.2544	0.0022	10,997	137

Table 2 Calibrated ^{14}C results—biannual data. *(Continued)*

Lab # AA-	Sample ID	δ^{13}C	^{230}Th age	±2 σ	F	±1 σ	F_{RC}	±1 σ	^{14}C age BP	±2 σ
AA52852	PNG 96 41.27 73L	–0.5	13,026.0	30.0	0.2457	0.0035	0.2585	0.0038	10,868	235
AA52853	PNG 96 41.27 74D	–0.4	13,025.5	30.0	0.2509	0.0027	0.2639	0.0030	10,700	181
AA52854	PNG 96 41.27 74L	–0.5	13,025.0	30.0	0.2405	0.0019	0.2530	0.0022	11,040	137
AA52855	PNG 96 41.27 75D	–1.2	13,024.5	30.0	0.2403	0.0016	0.2528	0.0019	11,047	119
AA52856	PNG 96 41.27 75L	–1.4	13,024.0	30.0	0.2392	0.0024	0.2516	0.0027	11,084	169
AA52857	PNG 96 41.27 76D	–0.6	13,023.5	30.0	0.2401	0.0014	0.2526	0.0017	11,054	107
AA52858	PNG 96 41.27 76L	–0.1	13,023.0	30.0	0.2399	0.0016	0.2524	0.0019	11,060	119
AA52859	PNG 96 41.27 77D	0.0	13,022.5	30.0	0.2460	0.0014	0.2588	0.0017	10,859	105
AA52860	PNG 96 41.27 77L	–0.1	13,022.0	30.0	0.2392	0.0026	0.2516	0.0029	11,084	182
AA52861	PNG 96 41.27 78D	–0.6	13,021.5	30.0	0.2410	0.0011	0.2535	0.0014	11,024	90
AA52862	PNG 96 41.27 78L	–0.5	13,021.0	30.0	0.2399	0.0016	0.2524	0.0019	11,060	119
AA52863	PNG 96 41.27 79D	–0.8	13,020.5	30.0	0.2411	0.0013	0.2536	0.0016	11,020	101
AA52864	PNG 96 41.27 79L	0.0	13,020.0	30.0	0.2438	0.0013	0.2565	0.0016	10,931	100
AA52865	PNG 96 41.27 80D	–0.9	13,019.5	30.0	0.2414	0.0016	0.2539	0.0019	11,010	119
AA52866	PNG 96 41.27 80L	–0.3	13,019.0	30.0	0.2406	0.0018	0.2531	0.0021	11,037	131
AA52867	PNG 96 41.27 81D	–0.1	13,018.5	30.0	0.2431	0.0016	0.2557	0.0019	10,954	118
AA52868	PNG 96 41.27 81L	–0.9	13,018.0	30.0	0.2436	0.0034	0.2563	0.0037	10,937	230
AA52869	PNG 96 41.27 82D	–0.4	13,017.5	30.0	0.2469	0.0050	0.2597	0.0053	10,829	329
AA52870	PNG 96 41.27 82L	0.5	13,017.0	30.0	0.2441	0.0017	0.2568	0.0020	10,921	123
AA52871	PNG 96 41.27 83D	0.0	13,016.5	30.0	0.2518	0.0057	0.2649	0.0061	10,671	367
AA52872	PNG 96 41.27 83L	0.1	13,016.0	30.0	0.2482	0.0051	0.2611	0.0054	10,787	334
AA52873	PNG 96 41.27 84D	–0.5	13,015.5	30.0	0.2515	0.0035	0.2646	0.0038	10,681	230
AA52874	PNG 96 41.27 84L	–0.3	13,015.0	30.0	0.2397	0.0028	0.2522	0.0031	11,067	195
AA52875	PNG 96 41.27 85D	0.0	13,014.5	30.0	0.2486	0.0014	0.2615	0.0017	10,774	104
AA52876	PNG 96 41.27 85L	–1.5	13,014.0	30.0	0.2399	0.0021	0.2524	0.0024	11,060	150
AA52877	PNG 96 41.27 86D	–2.0	13,013.5	30.0	0.2403	0.0021	0.2528	0.0024	11,047	150
AA52878	PNG 96 41.27 86L	–2.1	13,013.0	30.0	0.2422	0.0030	0.2548	0.0033	10,984	206
AA52879	PNG 96 41.27 87D	–2.0	13,012.5	30.0	0.2316	0.0023	0.2436	0.0025	11,343	168
AA52880	PNG 96 41.27 87L	–1.9	13,012.0	30.0	0.2423	0.0029	0.2549	0.0032	10,980	199
AA52881	PNG 96 41.27 88D	–1.5	13,011.5	30.0	0.2348	0.0019	0.2470	0.0022	11,233	140
AA52882	PNG 96 41.27 88L	–1.0	13,011.0	30.0	0.2407	0.0019	0.2532	0.0022	11,034	137

Table 3 5-yr weighted average values: F_{RC}, ^{14}C age BP, and Δ^{14}C.[a]

^{230}Th age BP	±2 σ	F_{RC}	±2 σ	n[b]	^{14}C age BP	±2 σ	Δ^{14}C (‰)	±2 σ
13,015	30	0.2541	0.0018	10	11,031	121	222.9	21.2
13,020	30	0.2525	0.0018	10	10,955	82	235.2	9.7
13,025	30	0.2537	0.0014	10	11,009	44	227.8	6.8
13,030	30	0.2548	0.0028	10	11,005	76	229.0	10.6
13,035	30	0.2504	0.0020	10	10,958	82	237.0	14.5
13,040	30	0.2507	0.0014	10	11,085	51	218.4	6.8
13,045	30	0.2524	0.0026	10	11,069	76	221.5	11.6
13,050	30	0.2520	0.0014	10	11,114	38	215.5	5.8
13,055	30	0.2506	0.0012	10	11,066	45	223.5	5.8
13,060	30	0.2529	0.0024	10	11,066	83	224.2	12.6
13,065	30	0.2514	0.0016	10	11,117	45	217.2	5.8
13,070	30	0.2557	0.0026	10	11,130	64	216.0	8.8
13,075	30	0.2540	0.0024	10	10,949	88	244.4	11.7
13,080	30	0.2541	0.0014	10	11,024	44	233.5	6.8
13,085	30	0.2576	0.0026	10	11,075	57	226.5	6.8
13,090	30	0.2505	0.0038	6	11,094	58	224.3	9.7

[a]Weighted averages were computed with the formulae of Bevington and Robinson (1992).
[b]n is the number of individual samples used to compute the weighted average.

Figure 3 shows the 5-yr weighted averages of the ^{14}C dates versus ^{230}Th ages. The trend of the data is rather flat, with some intra-decadal variability. Weighted average) ^{14}C values are plotted against the ^{230}Th ages in Figure 4. This data also show intra-decadal variability with a small peak in Δ^{14}C at about 13,075 BP. The gross trend in Δ^{14}C shows a modest increase with increasing age over the entire period.

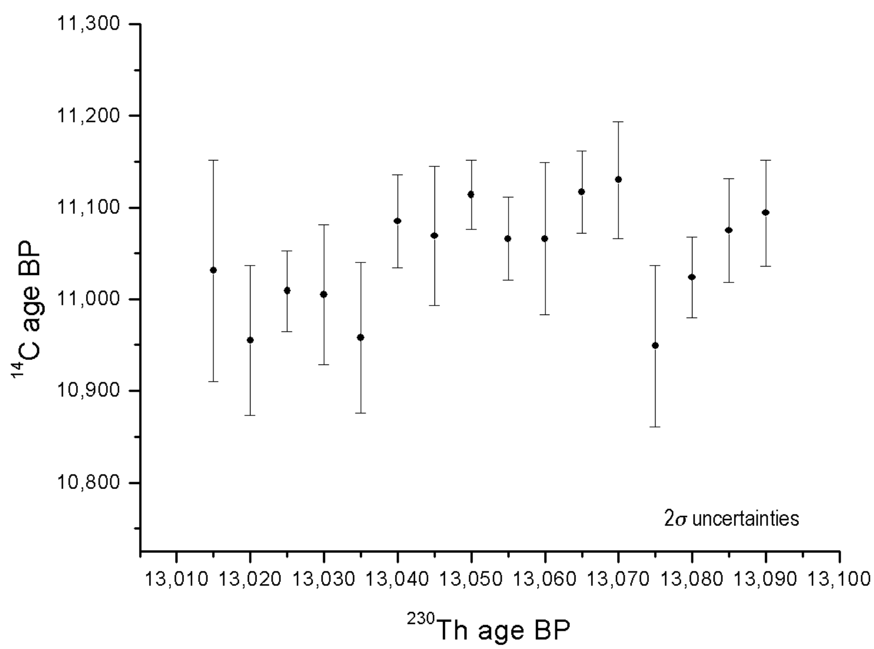

Figure 3 ^{14}C age versus ^{230}Th age: 5-yr averaged data

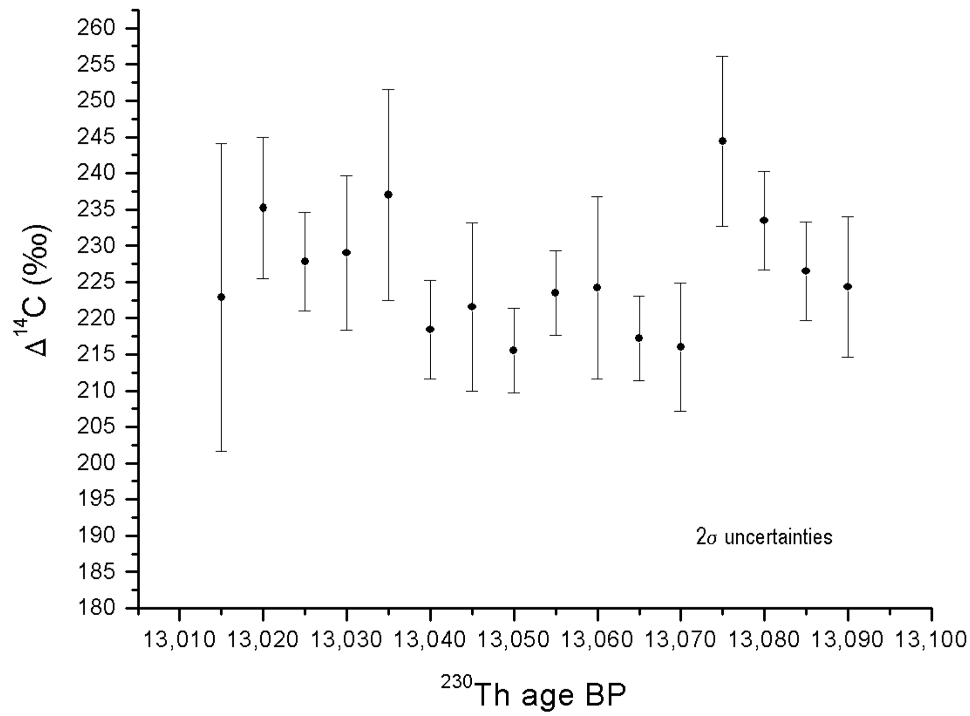

Figure 4 $\Delta^{14}C$ versus ^{230}Th age: 5-yr averaged data

Figure 5 shows a comparison of the results of this study with the earlier *Diploastrea* results. The ^{14}C age data and $\Delta^{14}C$ values from both corals follow a single trend. Note that the site-specific reservoir corrections for these 2 sites are different by about 90 yr.

An interesting feature of these results is the finestructure which can be seen in Figure 6. Here, we plot a 5-point smoothed curve for all of the data. The smoothed curve shown in the figure shows variability in $\Delta^{14}C$ with a frequency on the order of 4 to 10 yr and variable amplitudes of up to 40‰. These variations are similar to those observed in modern corals whose ^{14}C content has been shown to be related to El Niño-induced fluctuations (Brown et al. 1993; Guilderson and Schrag 1998). Such effects are also known to produce oxygen isotopic variations and these have been described from modern corals in Papua New Guinea (Tudhope et al. 2001). The oxygen isotope record of the *Goniastrea favulus* sample studied here, and the potential for paleo-El Niño events, is the subject of a parallel study to be discussed elsewhere.

CONCLUSIONS

This study highlights the advantages of analyzing consecutive subannual growth layers of a single coral, which allows annual variations in $\Delta^{14}C$ to be identified for the better part of a century. Intra-decadal $\Delta^{14}C$ variations between 13.0 and 13.1 kyr BP show variations which are similar to those observed in living corals. The time resolution of the sampling provides for the most precise ^{14}C results available for this period and the internal consistency of the results supports the quoted precision for the measurements. Using individual growth bands, 5-yr average values for the ^{14}C calibration have been computed here using 10 independent measurements, and the external variance of this population of points determines the precision of the calibrated age. Coral samples of the type examined here are difficult to sample in practice, but their usefulness for calibration purposes warrants further efforts to collect them.

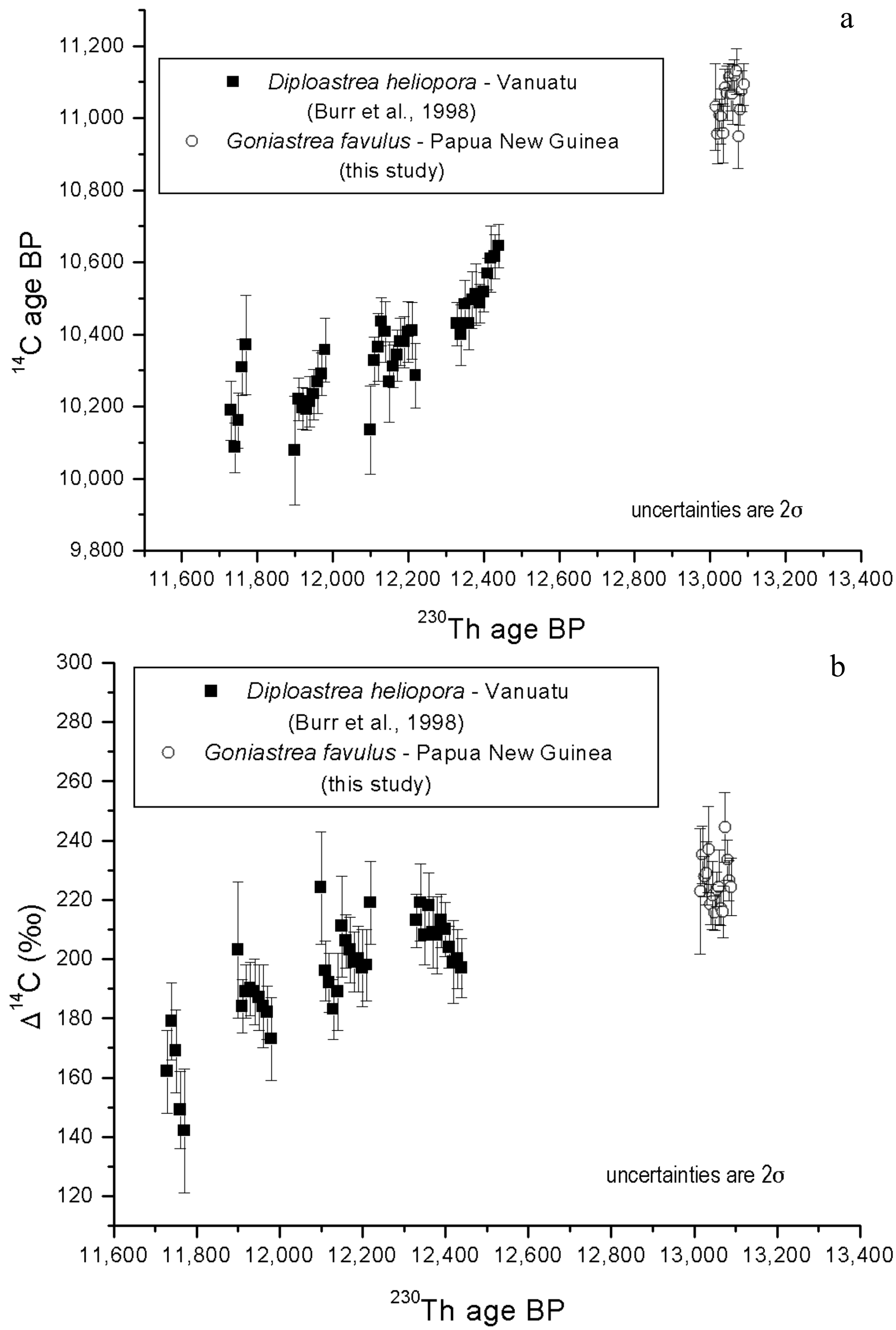

Figure 5 Comparison of Vanuatu and PNG results: (a) ^{14}C age versus ^{230}Th age; (b) $\Delta^{14}C$ versus ^{230}Th age. *Diploastrea* (Vanuatu) are 10-yr averages and *Goniastrea* (Papua New Guinea) are 5-yr averages.

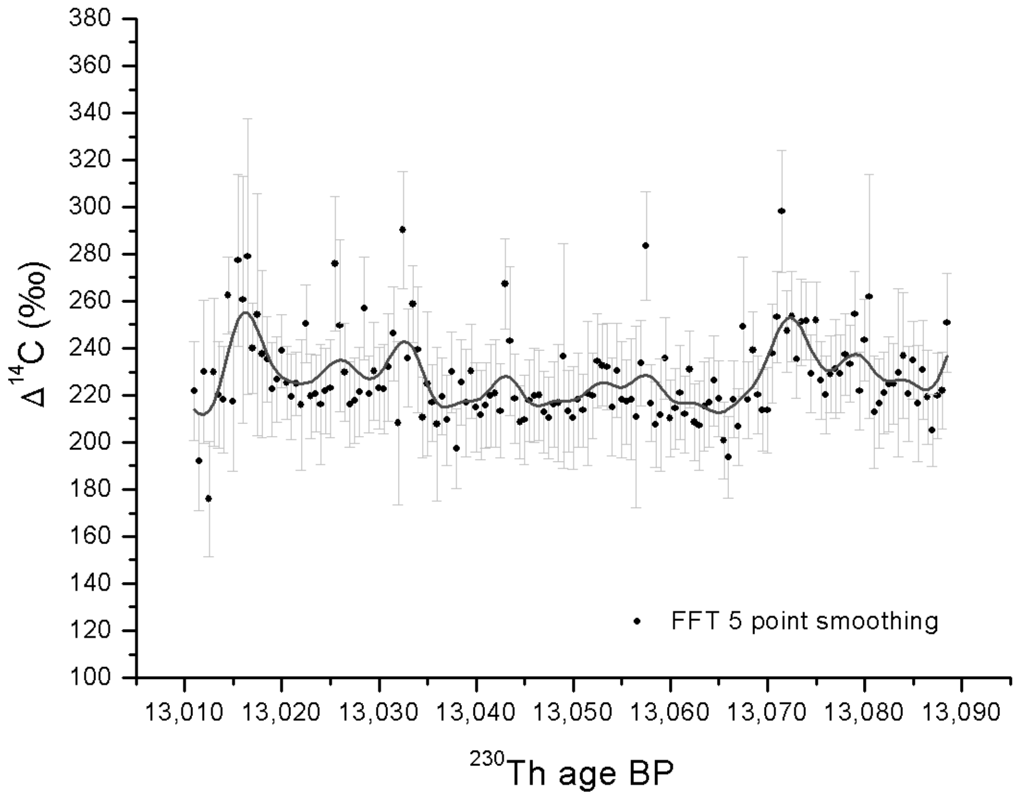

Figure 6 Finestructure in the *Goniastrea favulus* record: 5-point FFT smoothed curve

ACKNOWLEDGMENTS

We acknowledge the support for this project from the National Science Foundation (EAR9730699 and EAR0115488). We are very grateful for the enthusiastic support of the local inhabitants of Kwambu Village and of the support of the Sialum District government. We would like to thank Damien Kelleher and Eugene Wallensky of the Australian National University for their drilling expertise. We are also indebted to Dr John Chappell for making available the drilling equipment.

REFERENCES

Bard E, Hamelin B, Fairbanks RG, Zindler A. 1990. Calibration of the ^{14}C time scale over the past 30,000 years using mass spectrometric U-Th ages from Barbados corals. *Nature* 345:405–10.

Bard E, Arnold M, Fairbanks RG, Hamelin B. 1993. ^{230}Th-^{234}U and ^{14}C ages obtained by mass spectrometry on corals. *Radiocarbon* 35(1):191–9.

Bard E, Hamelin B, Arnold M, Montaggioni L, Cabioch G, Faure G, Rougerie F. 1996. Deglacial sea-level record from Tahiti corals and the timing of global meltwater discharge. *Nature* 382:241–4

Bevington PR, Robinson DK. 1992. *Data Reduction and Error Analysis for the Physical Sciences*. New York: McGraw-Hill, Inc. 328 p.

Brown TA, Farwell GW, Grootes PM, Schmidt FH, Stuiver M. 1993. Intra-annual variability of the radiocarbon content of corals from the Galapagos Islands. *Radiocarbon* 35(2):245–51.

Burr GS, Edwards RL, Donahue DJ, Druffel ERM, Taylor FW. 1992. Mass spectrometric ^{14}C and U-Th measurements in coral. *Radiocarbon* 34(3):611–8.

Burr GS, Beck JW, Taylor FW, Récy J, Edwards RL, Cabioch G, Corrège T, Donahue DJ, O'Malley JM. 1998. A high-resolution radiocarbon calibration between 11,700 and 12,400 calendar years BP derived from ^{230}Th ages of corals from Espiritu Santo Island, Vanuatu. *Radiocarbon* 40(3):1093–105.

Cabioch G, Banks-Cutler K, Beck JW, Burr GS, Corrège

T, Edwards RL, Taylor FW. 2003. Continuous reef growth during the last 23 cal kyr BP in a tectonically active zone (Vanuatu, southwest Pacific). *Quaternary Science Reviews* 22:1771–86.

Chappell J, Polach H. 1991. Post-glacial sea-level rise from a coral record at Huon Peninsula, Papua New Guinea. *Nature* 349:147–9.

Cutler KA, Edwards RL, Taylor FW, Cheng H, Adkins J, Gallup CD, Cutler PM, Burr GS, Bloom AL. 2003. Rapid sea-level fall and deep-ocean temperature change since the last interglacial period. *Earth and Planetary Science Letters* 206:253–71.

Donahue DJ, Linick TW, Jull AJT. 1990. Isotope-ratio and background corrections for accelerator mass spectrometry radiocarbon measurements. *Radiocarbon* 32(2):135–42.

Druffel ERM. 1997. Geochemistry of corals: proxies of past ocean chemistry, ocean circulation, and climate. *Proceedings National Academy of Sciences* 94:8354–61.

Edwards RL, Beck JW, Burr GS, Donahue DJ, Chappell JMA, Bloom AL, Druffel ERM, Taylor FW. 1993. A large drop in atmospheric $^{14}C/^{12}C$ and reduced melting in the Younger Dryas, documented with ^{230}Th ages of corals. *Science* 260:962–8.

Gagan MK, Ayliffe LK, Beck JW, Cole JE, Druffel ERM, Dunbar RB, Schrag DP. 2000. New views of tropical paleoclimates from corals. *Quaternary Science Reviews* 19:45–64.

Guilderson TP, Schrag DP, Kashgarian M, Southon J. 1998. Radiocarbon variability in the western equatorial Pacific inferred from a high-resolution coral record from Nauru Island. *Journal of Geophysical Research-Oceans* 103(C11):24,641–50.

Guilderson TP, Schrag DP. 1998. Abrupt shift in subsurface temperatures in the tropical Pacific associated with changes in El Niño. *Science* 281:240–3.

Moore MD, Schrag DP, Kashgarian M. 1997. Coral radiocarbon constraints on the source of the Indonesian throughflow. *Journal of Geophysical Research* 102(C6):12,359–65.

Reimer PJ, Baillie MGL, Bard E, Bayliss A, Beck JW, Blackwell PG, Buck CE, Burr GS, Cutler KB, Damon PE, Edwards RL, Fairbanks RG, Friedrich M, Guilderson TP, Herring C, Hughen KA, Kromer B, McCormac G, Manning S, Bronk Ramsey C, Reimer RW, Remmele S, Southon JR, Stuiver M, Talamo S, Taylor FW, van der Plicht J, Weyhenmeyer CE. 2004. IntCal04 terrestrial radiocarbon age calibration, 0–26 cal kyr BP. *Radiocarbon*, this issue.

Stuiver M, Reimer PJ, Bard E, Beck JW, Burr GS, Hughen KA, Kromer B, McCormac G, van der Plicht J, Spurk M. 1998. IntCal98 radiocarbon age calibration, 24,000–0 cal BP. *Radiocarbon* 40(3):1041–83.

Taylor FW, Frohlich C, Lecolle J, Strecker M. 1987. Analysis of partially emerged corals and reef terraces in the central Vanuatu arc: comparison of contemporary coseismic and nonseismic with Quaternary vertical movements. *Journal of Geophysical Research* 92: 4905–33.

Tudhope AW, Chilcott CP, McCulloch MT, Cook ER, Chappell J, Ellam RM, Lea DW, Lough JM, Shimmield GB. 2001. Variability in the El Niño-Southern Oscillation through a glacial-interglacial cycle. *Science* 291:1511–7.